

Thermopower and resistivity behavior in Ce-based Kondo-lattice systems: A phenomenological approach

C. S. Garde and J. Ray

Low Temperature Physics Group, Tata Institute of Fundamental Research, Homi Bhabha Road, Bombay 400005, India

(Received 26 September 1994)

A phenomenological model for understanding the thermopower S and the electrical resistivity ρ behavior of Ce-based Kondo-lattice systems is described. In this model, the low-temperature S and ρ behavior is critically governed by the position of the $4f$ density of states near the Fermi level E_F . The peak in the $4f$ density of states is centered at an energy $k_B T_0$ near E_F . In contrast to earlier studies, in the present model T_0 is temperature dependent and consequently leads to a better understanding of the low-temperature S behavior in many Kondo-lattice systems.

Ce-based Kondo-lattice (KL) systems have been the subject of active study¹⁻⁶ for more than a decade due to their complex magnetic behavior. These systems are characterized by the observation of large values of the coefficient γ of the electronic specific heat, the magnetic susceptibility χ , and also of the thermopower S . These quantities are typically 10–100 times larger than those for a simple metal like Cu, which indicates the presence of a large value for the density of states $N(E_F)$ at the Fermi energy E_F . Photoemission spectroscopy (PES) and inverse photoemission spectroscopy (IPES) data^{3,7-10} support this. However, the exact origin for the occurrence of a large $N(E_F)$ is still largely a matter of debate.⁷⁻¹⁰ PES studies⁹ suggest that it can result from the hybridization of the $4f$ and the conduction electrons at E_F even when the Kondo interaction is not important, whereas some other reports^{7,10-14} suggest that Kondo-type processes are important. In the Kondo-type models, a sharp many-body effect, commonly referred to as Abrikosov-Suhl resonance, arises out of the Kondo interaction of the conduction electrons with the $4f$ electrons of the Ce ions. This resonance peak is located near the Fermi level E_F . It has a width³ of the order of the characteristic Kondo temperature T_K . Despite the fact that this linewidth, in many systems, is smaller (< 0.01 eV) than the resolution limit (0.5 eV) presently achieved by PES and IPES experiments (and therefore cannot be detected directly), indirect evidence^{7,10-12} does seem to suggest the presence of such a peak, at E_F , in many Ce, Yb, and U compounds.

Amongst the transport experiments, the S measurement is of particular interest because it is extremely sensitive to any variation of $N(E_F)$. Typically, the S behavior of Ce-based KL systems exhibits large values (10–100 $\mu\text{V}/\text{K}$) and extremum features especially at low temperatures. These compounds can be broadly divided into two categories. In the first category, compounds like CeCu_2Si_2 , CeAl_3 , and CeAl_2 exhibit^{3,15} (Fig. 1) a broad positive maximum S_{max} (≈ 10 $\mu\text{V}/\text{K}$) at temperatures T_{max} (≈ 100 K), followed by a negative minimum S_{min} (≈ -10 $\mu\text{V}/\text{K}$) at T_{min} (≈ 10 K). The electrical resistivity ρ curve, on the other hand, shows a precipitous drop

at still lower temperatures ($T < T_{\text{min}}$) signifying the onset of coherence effects. At high temperatures, like S_{max} , ρ_{max} also is usually observed, at $T_{\text{max}} \approx 200$ K, due to crystal-field (CF) effects. The average separation Δ_{CF} of

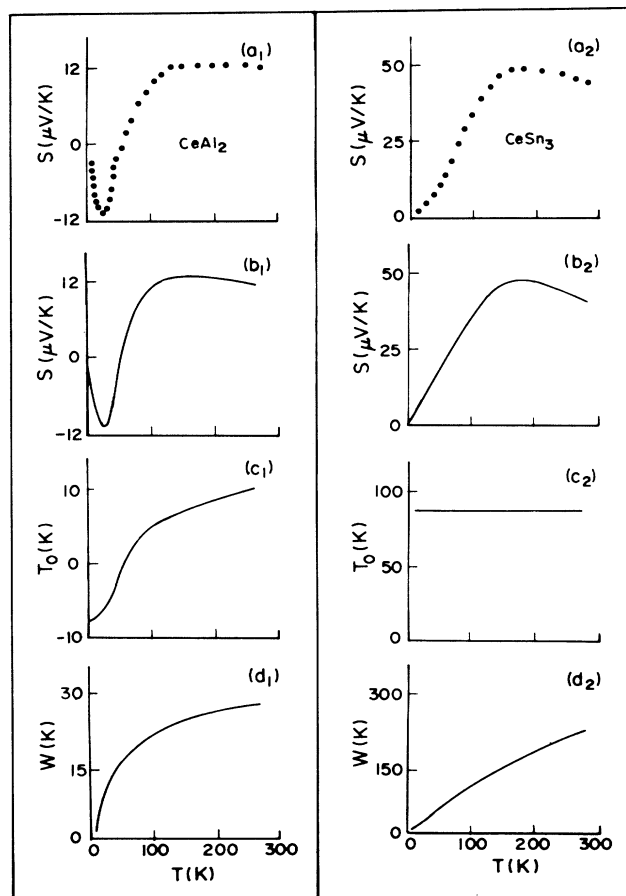


FIG. 1. S versus T curves for KL systems. Experimental curves (Refs. 3,15): a_1 , low- T_K compound CeAl_2 ; a_2 , high- T_K compound CeSn_3 . Simulated S curves: b_1 , CeAl_2 ; b_2 , CeSn_3 . T_0 versus T curves: c_1 , CeAl_2 ; c_2 , CeSn_3 . W versus T curves: d_1 , CeAl_2 ; d_2 , CeSn_3 .

these CF-split levels, for the Ce ions, is of the order of 200–300 K. In the second category, compounds like CePd₃, CeSn₃, and CeIn₃ exhibit (Fig. 1) only S_{\max} at T_{\max} . No extremum features are observed at low temperatures. The ρ curve also exhibits neither the sharp drop at low temperatures nor the high-temperature maximum. It is interesting to note that the first class of compounds usually have $T_K < \Delta_{\text{CF}}$, and these systems usually exhibit fixed valency for the Ce ion with heavy-fermion (HF) behavior, whereas the second class of compounds is characterized by $T_K \geq \Delta_{\text{CF}}$ and many of them show mixed-valent (MV) behavior. Though the phenomenon of S_{\max} at T_{\max} can be understood^{16,17} on the basis of a Kondo-type model with CF excitations, the precise origin of the negative S_{\min} at T_{\min} is still not clear. It has been argued¹⁸ that it arises from a Kondo-like process influenced by intersite effects. There is therefore an urgent need to understand this effect. We have attempted to understand, on the basis of a phenomenological model, especially the low-temperature S_{\min} and the ρ behavior in such KL systems.

The dominant contribution to the S value arises due to the scattering between the electrons in the broad $5d-6s$ conduction band and those in the narrow Lorentzian-shaped¹⁹ $4f$ band. The density of states of this band could be expressed as $N(E) = W/(T_0^2 + W^2)$, where W and T_0 represent the width and the position of the band. As S is proportional to the energy derivative (of the logarithm) of $N(E_F)$, the contribution to S from this narrow band has been taken¹⁹ proportional to $T_0/(T_0^2 + W^2)$. Therefore the total S could then be expressed¹⁹ as

$$S = C_1 T + \frac{C_2 T T_0}{T_0^2 + W^2}, \quad (1)$$

where

$$W = T_f \exp(-T_f/T). \quad (2)$$

C_1 and C_2 are temperature-independent parameters which determine the strength of the contributions from the nonmagnetic and magnetic scattering processes, respectively. T_f is a temperature-dependent parameter and is equated¹⁹ to the quasielastic linewidth, obtained from neutron studies, arising from the hybridization between the $4f$ electrons (forming a narrow band) and the surrounding conduction electrons (forming a broad band). W is proportional¹⁹ to the number of states in the peak that would effectively take part in the scattering process. Thus for $T \gg T_f$, $W = T_f$ and this indicates that all those states in the peak near E_F contribute to the scattering process, while for $T < T_f$, $W < T_f$, which implies that only a fraction of the states contributes to the scattering process.

In this model,¹⁹ $k_B T_0 = (E_F - E_f)$, where E_f is the energy corresponding to the center of gravity (CG) of the $4f$ peak in the density of states at E_F . k_B is the Boltzmann constant. Thus T_0 can be positive or negative depending on whether E_f is less than or greater than E_F , respectively. We note that in the earlier studies¹⁹ T_0 was taken to be temperature independent, whereas in our ap-

proach, the CG of the $4f$ peak is temperature dependence and T_0 now depends on temperature through the following equation:

$$T_0 = A + B \exp(-T_m/T). \quad (3)$$

A , B , and T_m are constants for a given alloy. At low temperatures ($T \ll T_m$), $T_0 \sim A$ [Eq. (3)]. This situation corresponds to Kondo scattering from the Ce ions in their low-temperature CF ground state, characterized by the total angular momentum $J = \frac{1}{2}$. At high temperatures ($T \gg T_m$), $T_0 \sim A + B$. At these temperatures, the Kondo scattering from the Ce ion occurs from all its populated CF-split levels, leading to the full value of $J = \frac{5}{2}$. Thus T_m plays the role of an important characteristic temperature scale in our model calculations. The exponential term [Eq. (3)] could thus represent, phenomenologically, the gradual filling up of the excited CF levels with increase of temperature.

The important aspects of our calculations are shown (Fig. 1) for the case of (1) a typical low- T_K (~ 10 K) compound like CeAl₂ and (2) a typical high- T_K (~ 300 K) MV compound like CeSn₃. The simulated curves (Fig. 1, curves b_1 and b_2) show close resemblance with their corresponding experimental curves¹⁵ (Fig. 1, curves a_1 and a_2). The temperature dependence (Fig. 1, curves c_1 and c_2) for the parameter T_0 for the above two classes of compounds is found to be quite different. A striking observation (Fig. 1) is that, for a low- T_K compound (like CeAl₂), T_0 and S both change sign (Fig. 1, curves a_1 and c_1) at approximately the same temperature. It is important to note that both the low-temperature S_{\min} behavior and the crossover in the sign of the S value can be reproduced only by a temperature-dependent T_0 . This reproduction of the low-temperature S_{\min} behavior (in low- T_K systems) has not been achieved so far in any of the earlier studies to our knowledge. For the high- T_K compounds (like CeSn₃), on the other hand, where there is neither the S_{\min} feature nor the crossover in the sign of the S value with temperature, T_0 is temperature independent.

The temperature dependence (Fig. 1, curves d_1 and d_2) of W for the above class of compounds is, however, not so different from that found for T_0 . The W curves display a monotonic increase with temperature. For computing the value of W , the values of T_f have been taken equal to the quasielastic linewidths (for $4.2 < T < 300$ K) obtained^{20–23} from neutron studies. For CeAl₂, T_f has a monotonically increasing temperature dependence,^{20–23} whereas for CeSn₃ T_f is temperature independent and is equal to 300 K.

At low temperatures ($T < 50$ K), the S behavior is mainly influenced by the second term in Eq. (1). At the lowest temperatures ($T \rightarrow 0$), $W \ll T_0$, $T_0 \sim A$, and hence we have $S \propto T/A$ [from Eqs. (1)–(3)]. Thus in our model the value of A has been determined by the initial slope of the experimental S curve. At higher temperatures ($T > 50$ K), both A and the exponential term [of Eq. (3)] contribute to T_0 . In this temperature range, the simulated S curves match the experimental curves by appropriate choice of B and T_m . The S_{\max} (Fig. 1) at T_{\max} (~ 150

TABLE I. Various parameters obtained from the simulation studies. The references to experiments of different authors are indicated. The experiments on the $\text{Ce}(\text{Cu}_{1-x}\text{Ni}_x)_2\text{Si}_2$ system pertain to the present work.

Compound	C_1 ($\mu\text{V}/\text{K}^2$)	C_2 ($\mu\text{V}/\text{K}$)	T_m (K)	A (K)	B (K)	T_0 (K)	ρ_0 ($\mu\Omega\text{ cm}$)	a ($\mu\Omega\text{ cm}/\text{K}$)	E ($\mu\Omega\text{ cm K}$)
CeAl_2^{a}	-0.05	39.8	99	-8.8	11.8				
CeSn_3^{a}	-0.07	37.8	0	83.0		83			
$\text{Ce}(\text{Cu}_{1-x}\text{Ni}_x)_2\text{Si}_2$									
$x=0$	-0.15	23.5	230	-10.0	160		72.83	0.12	1138
0.03	-0.06	13.3	200	-8.0	150		98.74	0.08	1618
0.07	-0.13	20.5	200	0.5	140		92.35	0.02	1924
0.10	-0.11	42.5	30	10.0	52		101.2	0.01	4518
0.15	-0.26	42.8	20	11.0	50		176.0	0.01	3129
0.4	-0.17	40.5	0	35.0		35	205.6	0.02	6184
0.65	-0.12	45.0	0	130.0		130	158.5	0.25	3337
1	-0.005	15.7	0	150.0		150	68.0	0.22	2956
$\text{CePd}_2\text{Si}_2^{\text{b}}$	-0.23	17.0	116	-2.0	89.0				
CeIn_3^{c}	-0.17	35.0	0	40.0		40			

^aReference 15.

^bReference 25.

^cReference 26.

K) occurs when the first term [in Eq. (1)] becomes comparable to the second term and C_1 and C_2 have opposite signs (Table I).

Using the above simulation procedure, we have also investigated the well-known $\text{Ce}(\text{Cu}_{1-x}\text{Ni}_x)_2\text{Si}_2$ series. The S and ρ measurements have been carried out by us in the temperature interval of 1.7 and 300 K. In this series, the HF phase (low $T_K \approx 10$ K) crosses over to the MV phase (high $T_K \approx 300$ K) for $x > x_c$ (~ 0.40). For the $x=0$ and $x=1$ compounds, the temperature dependence of T_f is deduced²⁰⁻²³ from the quasielastic linewidth data. For the $x=0$ case (low $T_K \approx 10$ K), T_f is a monotonically increasing function²⁰⁻²³ of temperature ($T_f=10$ K for $T=1.2$ K and 70 K for $T=300$ K), whereas, for the $x=1$ case (high $T_K \approx 300$ K), T_f is temperature independent ($T_f=300$ K). For the other alloys ($0 < x < 1$), T_f , at any given temperature, is obtained by linearly interpolating the corresponding T_f values for the $x=0$ and the $x=1$ compounds. Our simulation studies [Figs. 2(a) and 2(b)] show that, precisely at $x > x_c$, T_0 becomes temperature independent (Table I), whereas, for $x < x_c$, T_0 is strongly temperature dependent. This temperature independence of T_0 therefore serves as a useful criterion to distinguish the MV systems from the HF ones. For $x < x_c$, negative values of T_0 (Table I) are obtained with negative values of A and positive values of B and T_m . For example, for the simulated curve of the $x=0$ sample, $A = -10$ K, $B = 160$ K, and $T_m = 230$ K. Thus we have for $T=0$ $T_0 = A = -10$ K. We note that, for a given alloy concentration x , the values of the parameters A , B , and T_m all become temperature independent. With the above combination of A , B , and T_m , $T_0 \sim 0$ at $T=40$ K. This is quite close to the temperature (≈ 40 K) where the S curve changes sign from negative to positive. With such a choice of parameters, the simulated curves reproduce (Fig. 2) the low-temperature negative S_{\min} behavior clearly. At around 200 K, the simulated curve also

reproduces the broad maximum due to CF effects. At these elevated temperatures, $T_0 \approx 100$ K. We note that, for a given alloy, the total variation of T_0 with temperature is approximately about 100 K. This correspond to a shift of the narrow $4f$ resonance band (with respect to E_F) by about 10 meV. Such small changes in the position of the narrow $4f$ band are at present difficult¹⁰ to measure experimentally.

As the value of S_{\min} approaches zero [Fig. 2(a)] with increase in x , the value of A (Table I) changes (Fig. 3) from negative ($A = -10$ K, $x=0$) to positive ($A = 10$ K, $x=0.1$). On the other hand, the value of T_m (Table I) decreases rapidly (Fig. 3) from 230 K (for $x=0$) to 20 K (for $x=0.15$). S_{\min} moves (with increase in x) from a negative to a positive value and an additional peak is ob-

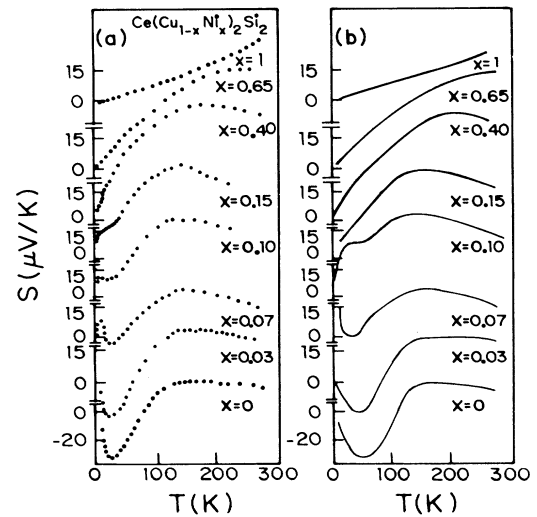


FIG. 2. S versus T curves for the $\text{Ce}(\text{Cu}_{1-x}\text{Ni}_x)_2\text{Si}_2$ systems. (a) experimental (this work) and (b) simulated.

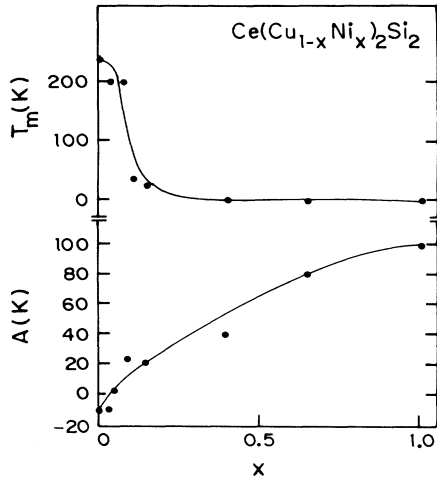


FIG. 3. Plots of A and T_m versus x for the $\text{Ce}(\text{Cu}_{1-x}\text{Ni}_x)_2\text{Si}_2$ system. The solid lines are hand drawn to guide the eyes.

served experimentally (Fig. 2) for $T < T_{\min}$. Such a positive peak may arise²⁴ due to the formation of a pseudogap in the $4f$ density of states. Our simulated curves (Fig. 4) also reproduce these experimental features quite well. As mentioned earlier, $S \propto T/A$ for $T \rightarrow 0$. As the value of A is positive (Table I) and small, the S curve has a positive value and increases rather sharply [Fig. 2(b)] as the temperature is increased from $T=0$. With further increase of T , the temperature-dependent term [in Eq. (3)] becomes comparable to A and hence the S value [Eq. (1)] decreases. Thus the curve goes through a maximum.

For $x \geq x_c$, the S_{\min} feature is no longer observed and the curve exhibits [Fig. 2(a)] a monotonic temperature dependence. Such a behavior can be reproduced [Fig. 2(b)] with $T_m \approx 0$ (Table I).

The simulated curves [Fig. 2(b)] thus reproduce the experimentally observed ones [Fig. 2(a)] for all the values of

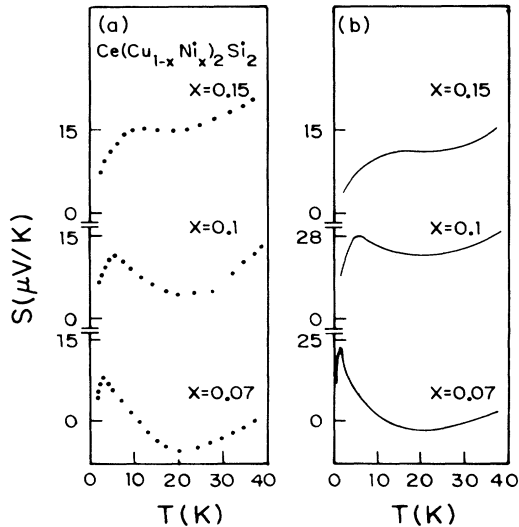


FIG. 4. Expanded plots of the low-temperature S behavior. (a) experimental (this work) and (b) simulated.

x in the $\text{Ce}(\text{Cu}_{1-x}\text{Ni}_x)_2\text{Si}_2$ series. We observe that the negative minimum in the simulated curves is relatively broad compared to that observed experimentally. However, all the *essential* features, namely, (a) the negative minimum at low temperatures, (b) the crossover to positive values at intermediate temperatures, and (c) the maximum at high temperatures, are reproduced in our model calculations.

The above analysis shows that when T_K is small (≈ 10 K) then for $x \leq x_c$, T_m is large and finite, whereas when T_K is large (≈ 200 K) for $x > x_c$, T_m tends to 0. We note that for low- T_K systems, when the broadening of the CF-split levels is small, the value of T_m agrees (within a factor of 2) with $\Delta_{\text{CF}} \approx 300$ K. In this low- T_K limit, where the CF-split levels are sharp, Eq. (3) rightly determines the gradual population of those states. The value of T_m ($\approx \Delta_{\text{CF}}$) thus serves as an indication for the effective separation between the CF-split levels. For the high- T_K systems ($x > x_c$), on the other hand, the CF levels overlap greatly due to level broadening. By the application of the above criterion, the value of T_m would tend to zero. As shown in our analysis, a low value of T_m is indeed reflected (Table I) for systems in the MV (high- T_K) regime ($x > x_c$). In the MV regime, $T_m \approx 0$ and as a consequence the exponential term [Eq. (3)] becomes unity and therefore T_0 also becomes temperature independent. Thus our simulation studies reveal that the magnitude of T_m also can serve as a useful criterion to distinguish between the HF and MV systems. This criterion has been tested, using this model, to hold good for other HF systems^{16,25} like CePd_2Si_2 ($T_K \approx 10$ K, $T_m = 116$ K) and CeAl_2 ($T_K \approx 2$ K, $T_m = 99$ K) where T_m turns out to have a large value (Table I), and MV systems²⁶ like CeSn_3 ($T_K \approx 300$ K, $T_m = 0$) and CeIn_3 ($T_K \approx 300$ K, $T_m = 0$) where T_m tends to zero (Table I).

Apart from the S behavior, our model can also simulate the ρ data in this class of compounds. Using similar intuitive arguments as employed for the derivation of S , the ρ contribution, arising from the scattering of electrons between the broad conduction band and the narrow Lorentzian-shaped $4f$ band, is proportional to $N(E_F) = W/(T_0^2 + W^2)$. The total contribution to ρ could then be written as¹⁹

$$\rho = \rho_0 + aT + E \frac{W}{T_0^2 + W^2}. \quad (4)$$

ρ_0 is the temperature-independent residual resistivity term and a is a constant which typifies the strength of the nonmagnetic phonon term. E is another constant which relates to the strength of the $4f$ band term. The other symbols have their meaning as explained earlier. The ρ data, exhibiting the low-temperature Kondo minimum and the sharp coherence drop ($T < T_K$) as well as the high-temperature CF-derived maximum, can all be reproduced (Fig. 5) by this model with the same value (Table I) of the parameters A , B , and T_m used for the S studies. The other additional parameters suitably chosen (Table I) are ρ_0 , a , and E . The introduction of a temperature-dependent T_0 , with the same value as in the S simulation studies, also reproduces both the low- and the high-

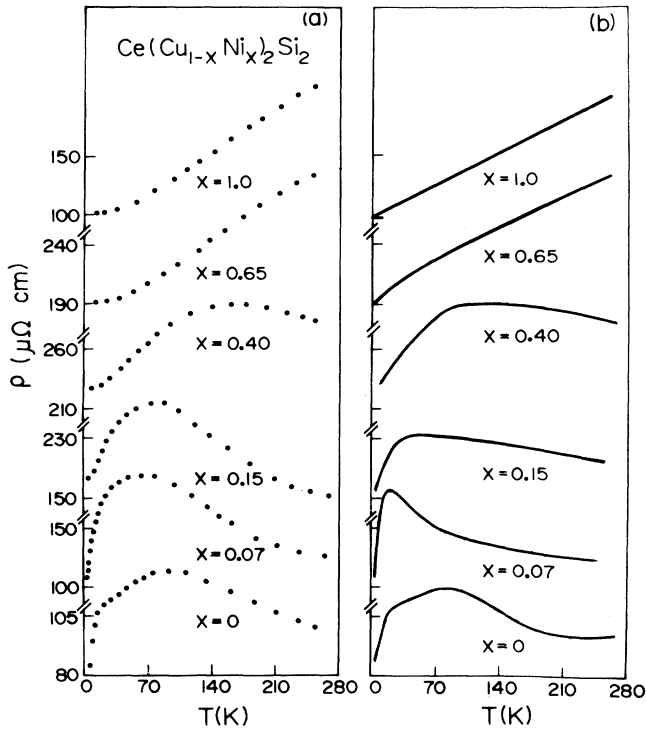


FIG. 5. ρ versus T curves for the $\text{Ce}(\text{Cu}_{1-x}\text{Ni}_x)_2\text{Si}_2$ system. (a) experimental (this work) and (b) simulated.

temperature features in the ρ curves of CeCu_2Si_2 (Fig. 5). We note that in the earlier study¹⁹ the ρ behavior, at high temperatures ($T > T_{\text{max}}$) only, could be reproduced with a temperature-independent T_0 . However, though our model reproduces the sharp drop in the ρ curve for $T < T_{\text{min}}$, it does not predict the power-law (T^2) behavior

for ρ (as $T \rightarrow 0$) that has been experimentally observed in many KL systems.

An important difference between the S and ρ behavior is that, while S [Eq. (1)] can take both positive and negative values, ρ [Eq. (4)] can take only positive values. We note that it has been possible to reproduce the change of sign of the value of S from negative at low temperatures ($T \leq T_{\text{min}}$) to positive at high temperatures. This is possible due to the fact that S is an odd function [Eq. (1)] of T_0 . We note that the sign of T_0 essentially indicates the relative position of the $4f$ band with respect to E_F . For example, in the simulation studies of $\text{Ce}(\text{Cu}_{1-x}\text{Ni}_x)_2\text{Si}_2$, for $x < x_c$, it is found that $T_0 < 0$ at low temperatures ($T \sim T_{\text{min}}$) whereas $T_0 > 0$ at high temperatures ($T \sim T_{\text{max}}$). The change of the sign of T_0 occurs (Fig. 1, curve c_1) over a narrow temperature range as shown for the typical case of CeAl_2 . This shows that with increase of temperature the $4f$ band moves from above to below E_F . This is one of the most important consequences of these model calculations. Though such a movement of the $4f$ band could be predicted from the S studies, the ρ studies are incapable of offering this information. This is because in the expression [Eq. (4)] for ρ T_0 appears as an even power. Thus the ρ behavior is insensitive to the sign of T_0 .

In conclusion, all the important experimentally observed features of the S and ρ curves of the Ce-based KL compounds could be reproduced in our model. Especially, the low-temperature S_{min} behavior has been successfully reproduced in our model simulations. The temperature dependence of T_0 is found to be a crucial factor in determining the low-temperature S behavior of these compounds. Finally, the values of both T_0 and T_m are quite different for the HF and MV compounds and could thus provide important signatures for the characterization of these exotic systems.

¹F. Steglich, J. Aarts, C. D. Bredl, W. Lieke, D. Meschede, W. Franz, and H. Schäfer, *Phys. Rev. Lett.* **43**, 1892 (1979).
²G. R. Stewart, *Rev. Mod. Phys.* **56**, 755 (1984).
³N. B. Brandt and V. V. Moshchalkov, *Adv. Phys.* **33**, 373 (1984).
⁴H. R. Ott, *Prog. Low Temp. Phys.* **11**, 215 (1987).
⁵P. Fulde, *J. Phys. F* **18**, 601 (1988).
⁶P. A. Lee, T. M. Rice, J. W. Serene, L. J. Sham, and J. W. Wilkins, *Comments Cond. Mat. Phys.* **12**, 99 (1986).
⁷S. Hüfner and L. Schlapbach, *Z. Phys. B* **64**, 417 (1986).
⁸T. Kashiwakura, S. Suzuki, T. Okane, S. Sato, T. Kinoshita, A. Kakizaki, T. Ishii, Y. Isikawa, H. Yamagami, and A. Hasegawa, *Phys. Rev. B* **47**, 6885 (1993).
⁹G. Kaindl, E. Weschke, C. Laubschat, R. Ecker, and A. Höhr, *Physica B* **186-188**, 44 (1993).
¹⁰D. Malterre, M. Grioni, P. Weibel, B. Dardel, and Y. Baer, *Phys. Rev. Lett.* **68**, 2656 (1992).
¹¹L. H. Tjeng, S. J. Oh, E. J. Cho, H. J. Lin, C. T. Chen, G. H. Gweon, J. H. Park, J. W. Allen, T. Suzuki, M. S. Kakivic, and D. L. Cox, *Phys. Rev. Lett.* **71**, 1419 (1993).

¹²M. Grioni, D. Malterre, P. Weibel, B. Dardel, and Y. Baer, *Physica B* **186-188**, 38 (1993).
¹³O. Gunnarson and K. Schönhammer, *Phys. Rev. B* **28**, 4315 (1983).
¹⁴O. Gunnarson and K. Schönhammer, in *Handbook on the Physics and Chemistry of Rare-Earths*, edited by K. A. Gschneidner, Jr., L. Eyring, and S. Hüfner (North-Holland, Amsterdam, 1987), Vol. 10, p. 103.
¹⁵D. Jaccard and J. Sierro, in *Valence Instabilities*, edited by P. Wachter and H. Boppert (North-Holland, Amsterdam, 1992), p. 409.
¹⁶A. K. Bhattacharjee and B. Coqblin, *Phys. Rev. B* **13**, 3441 (1976).
¹⁷S. Maekawa, S. Kashiba, M. Tachiki, and S. Takahashi, *J. Phys. Soc. Jpn.* **55**, 3194 (1986).
¹⁸K. H. Fischer, *Z. Phys. B* **76**, 315 (1989).
¹⁹A. Freimuth, *J. Magn. Magn. Mater.* **68**, 28 (1987).
²⁰L. C. Lopes, Y. Lassailly, R. Jullien, and B. Coqblin, *J. Magn. Magn. Mater.* **31-34**, 251 (1983).
²¹L. C. Lopes and B. Coqblin, *Phys. Rev. B* **38**, 6807 (1988).

- ²²S. Horn, F. Steglich, M. Lowenhaupt, and E. Holland-Moritz, *Physica B&C* **107B**, 103 (1981).
- ²³E. Holland-Moritz, D. Wohlleben, and M. Loewenhaupt, *Phys. Rev. B* **25**, 7482 (1982).
- ²⁴N. Grewe, *Solid State Commun.* **50**, 19 (1984).
- ²⁵A. Amato and J. Sierro, *J. Magn. Magn. Mater.* **47-48**, 526 (1985).
- ²⁶J. Sakurai, K. Murata, and Y. Komura, *Solid State Commun.* **49**, 287 (1984).